Carbohydrate Polymers 91 (2013) 224–228

Contents lists available at SciVerse ScienceDirect

Carbohydrate Polymers

journal homepage: www.elsevier.com/locate/carbpol

The preparation and characterization of liquefied wood based primary fibers

Jian Lin, Jun-Bo Shang, Guang-Jie Zhao*

College of Materials Science and Technology, Beijing Forestry University, Beijing 100083, PR China

ARTICLE INFO

Article history:
Received 26 June 2012
Received in revised form 17 July 2012
Accepted 3 August 2012
Available online 10 August 2012

Keywords:
Wood liquefaction
Primary fibers
Length/diameter ratio
Thermal stability
Porous structure
Hydrogen bond

ABSTRACT

The preparation of primary fibers were performed from liquefied wood in phenol by melt-spinning with different spinnerettes of length/diameter ratio (L/D) (0, 2, and 4), to investigate the effect of the size of spinnerette on the thermal stability and structural properties of primary fibers. High thermal transition temperatures and small weight loss percentages of resultant primary fibers representing good thermal stability were obtained with L/D of spinnerette increasing. Besides, few defective structure occurred on cross section and surface of primary fiber s in comparison with those prepared with spinnerette of $L/D = 0$. We found that these improvements were caused by the formation of hydrogen bond among phenolic hydroxyl groups in the period of flow entering the cylindrical die of spinnerette. Thus, the precursor, with either porous structure for preparing activated carbon fibers or defect-free structure for preparing carbon fibers with high performance, can be probably prepared by controlling the spinnerette system.

© 2012 Published by Elsevier Ltd.

1. Introduction

As typical biomass materials in nature, nowadays, both wood and its main components including cellulose, hemicelluloses, and lignin have attracted more and more attention concerning their effective utilization, due to the abundant and renewable characterization. Wood liquefaction, wherein wood flour is directly solvolyzed with the solvent of phenol or polyalcohol at the presence of small amount acid as catalyst, has been proved to be one of the effective techniques for preparing wood-based materials such as adhesives, foams, and moldings (Maldas, Shiraishi, & Harada, 1997; Lee, Teramoto, & Shiraishi, 2002; Lin, Yoshioka, Yao, & Shiraishi, 1995a, 1995b). Comparatively, preparation of carbon fibers (CFs) from liquefied wood seems to be a more facile and promising process because of higher value-added process (Ma & Zhao, 2010).

In general, the process for manufacturing CFs consists of several steps, such as wet or melt spinning depending on raw material, thermostabilized treatment for obtaining infusible fibers and carbonization in inert atmosphere at temperatures of 1000–2000 °C as well as the graphitization at 2000–3000 °C. As the first step, melt-spinning process, for mesophase pitch or liquefied wood as the starting material, is a key step to prepare excellent fibers for producing CFs with high performance. This step governs the macrostructure of spun fibers and eventually determines the texture and properties of resultant CFs through several important melt-spinning parameters (Zha, Shi, Ji, Liu, & Qian, 1992). Among these parameters, the size and shape of spinnerette plays a quite significant role in forming transverse structure of the filament which is formed by rearrangement of spinning solution through the spinnerette capillary during spinning (White & Buechler, 1984). Additionally, pitch-based CFs with random transverse structure are less graphitizable than that with radial transverse structure, and occasionally leads to the formation of defects along the filament axis, resulting in the great reduction of mechanical properties of CFs (Bright & Singer, 1979; Hamada, Nishida, Furuyama, & Tomioka, 1988). Therefore, more attention should be paid to these problems for obtaining the desirable products.

However, there were few investigations on reporting the effect of melt-spinning parameters on the quality of resultant liquefied-wood based primary fibers. Accordingly, in this article we describe the efforts directed at the characterization and evaluation of primary fibers derived from liquefied wood in phenol by melt-spinning with different spinnerettes.

2. Materials and methods

2.1. Preparation of liquefied wood based primary fibers

Twenty grams of dried Chinese Fir (*Cunninghamia lanceolata*) powder (20–80 mesh) were placed in a round bottom flask together with 120 g of phenol and 9.6 g of phosphoric acid (8 wt% on the weight of phenol). The flask was immersed in an oil bath that was preheated at 160 °C for 150 min. The flask was then cooled to room

---

* Corresponding author at: Laboratory of Wood Science, College of Materials Science and Technology, Beijing Forestry University, Qinghua East Road 35#, Haidian District, Beijing 100083, PR China. Tel.: +86 010 6233 6304; fax: +86 010 6233 7751.
E-mail address: zhaows@bjfu.edu.cn (G.-J. Zhao).

0144-8617/$ – see front matter © 2012 Published by Elsevier Ltd.
http://dx.doi.org/10.1016/j.carbpol.2012.08.007

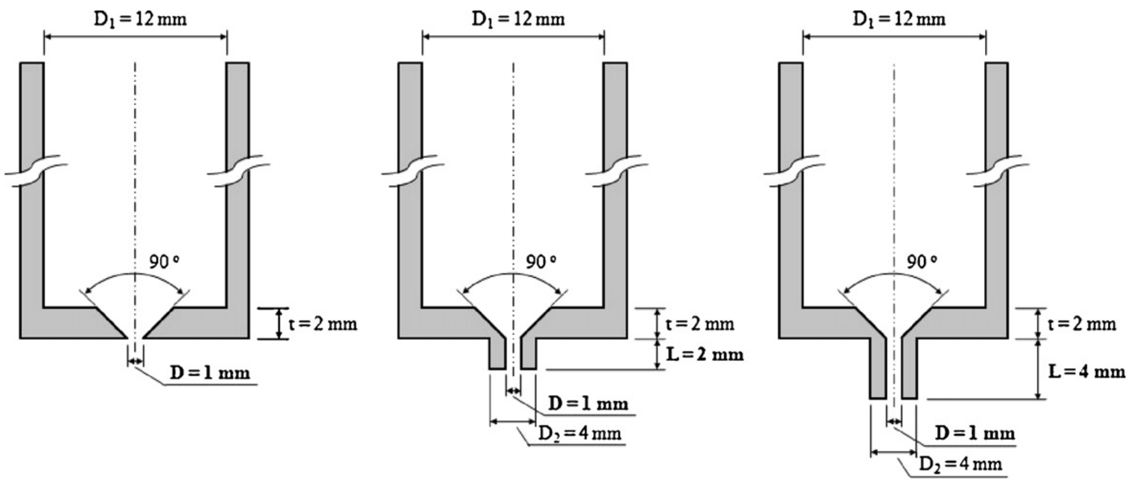

(A): L / D = 0 (B): L / D = 2 (C): L / D = 4

Fig. 1. Illustration of spinnerettes with different *L*/*D*.

temperature with cooling water, and then 0.75 L of acetone was added to the reaction product. The resultant mixture was filtrated through filter paper to separate filtrate and residue.

The acetone in the filtrate was removed by evaporation. The resulting liquefied wood mixed with hexamethylenetetramine (HMTA) (5 wt% on the weight of liquefied wood) were transferred into the metal tube equipped with different sizes of spinnerette [Length/Diameter ratio (*L*/*D*) = 0, 2, and 4] (as shown in Fig. 1). The mixture was heated from room temperature to 120 °C with the heating rate of 2.5 °C/min, and then the final temperature of 120 °C was maintained for 5 min to obtain the spinning solution. Subsequently, the melt-spinning process was conducted to prepare the primary fibers at the nozzle temperature of 120 °C and the winding rates of 14 m/min under a nitrogen pressure.

2.2. Characterizations

2.2.1. Thermogravimetry (TG)

The weight loss behaviors and decomposition temperature (T_d) of liquefied wood based primary fibers were measured by using thermogravimetric analysis (TGA) and differential thermal analysis (DTA) on a simultaneous thermal analyzer (DTG-60, Shimadzu, Japan) from room temperature to 600 °C with the heating rate of 10 °C/min in high pure nitrogen stream (30 mL/min).

2.2.2. Thermomechanical analysis (TMA)

TMA was performed on a TMA-4000S System (MAC Science System 010, MAC Science, Yokohama, Japan) at the temperature ranging from 30 to 300 °C under compression loading of 5 g under a N_2 stream at 0.15 L/min. The glass transition temperature (T_g) and thermal-flow starting temperature (T_f) were estimated as a first and a second transition points in TMA profiles (Kubo, Uraki, & Sano, 1996).

2.2.3. Scanning electronic microscopy (SEM)

Morphologies of primary fibers were observed by scanning electronic microscopy (SEM; S-3400N, Hitachi, Japan) using gold-coated samples, at magnification factors of 1500–5000, and at an accelerating voltage of 10 kV, respectively.

2.2.4. Fourier transform infrared spectroscopy (FTIR)

Fourier transform infrared (FTIR) spectroscopy was carried out on an FTIR spectrophotometer (TENSOR 27, Bruker, Germany), using the KBr disk method.

2.2.5. Mercury intrusion porosimetry (MIP)

Fiber pore structures were characterized by mercury porosimetry (AutoScan-33, Quantachrome, USA) with the pressure ranging from 0.2 to 60,000 psia and equilibration time of 10 s (Leon, 1998).

3. Results and discussion

3.1. Thermal stability of primary fibers

Melt-spinning processes were successfully conducted to prepare liquefied wood based primary fibers from spinning solution at 120 °C with different *L*/*D* spinnerettes. The primary fibers exhibited significant differences in thermal stability by TGA measurements as shown in Fig. 2. With the temperature increasing, all the primary fibers weights decreased to various degree, and the weight loss processes could be partitioned into two stages (stage 1: sharp weight loss varying from 150 °C to 400 °C; stage 2: slow weight loss ranging from 400 °C to 600 °C) excluding the temperature lower than 150 °C because of the loss of adsorbed water molecules, which derived from ambient environment.

In the case of stage 1, high weight loss process was mainly induced by the thermal degradation starting from the decomposition temperature (T_d), which was defined as a temperature that give a 5% weight loss (Uraki, Kubo, Nigo, Sano, & Sasaya, 1995). As shown in Table 1, high *L*/*D* of spinnerette gave rise to the high T_d of primary fibers. Especially for the *L*/*D* = 4, around 20 °C increase of T_d was obtained in comparison with that of primary fibers prepared with spinnerette of *L*/*D* = 0, resulting in the decrease of weight loss percentage from 39.2% to 33.3% in this stage. For stage 2, similarly, decrease in weight loss percentage took place with the *L*/*D* of spinnerette increasing, which was probably caused by the complete decomposition (Zheng, Zhou, Du, & Zhang, 2002). Accordingly, the highest residual ratio of 53.2% was obtained by using

Table 1
Thermal transition temperatures and residual ratio of primary fibers prepared with different *L*/*D* spinnerettes.

L/*D*	Transition temperature (°C)[a]			Residual ratio (%)
	T_g	T_f	T_d	
0	97	140	210	45.3
2	95	142	215	45.3
4	104	149	229	53.2

[a] T_g, T_f, and T_d denote glass transition temperature, thermal-flow starting temperature, and decomposition temperature, respectively.

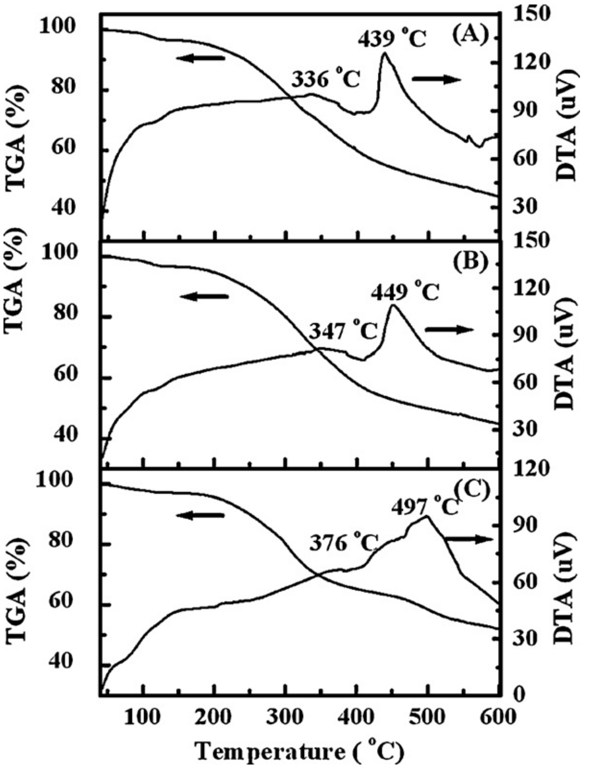

Fig. 2. TGA and DTA curves of primary fibers prepared from liquefied wood with different L/D spinnerettes. (Notes: (A) $L/D=0$; (B) $L/D=2$; (C) $L/D=4$).

the spinnerette with L/D of 4, indicating that the thermal stability of primary fibers could be improved via increasing L/D of spinnerette. Besides, the corresponding exothermic peaks occurred in DTA curves ranging from 336 °C to 376 °C and 439 °C to 497 °C with the L/D increasing (Fig. 2), suggesting that the TGA curves are in good agreement with the DTA results of these fibers.

Additionally, the glass transition temperature (T_g) and thermal-flow starting temperature (T_f) of the primary fibers were estimated by TMA, which was reported to be a suitable analytical method for thermal transition phenomena (Kubo et al., 1996). As shown in Fig. 3, TMA curves of primary fibers showed two transition points which corresponded to the T_g and T_f, respectively. Interestingly, the primary fiber prepared with spinnerette of $L/D=2$ showed the T_g of 94 °C (Table 1), which was little smaller than that of primary fiber prepared with spinnerette of $L/D=0$. In the case of T_f, the same increscent trend with that of T_d was obtained with the L/D increasing. However, there was only a few improvements in T_f of the fiber prepared with spinnerette of $L/D=2$ in comparison with that prepared with spinnerette of $L/D=0$, which was similar to the residual ratios results. Thus, the spinnerette with L/D of 2 may not fully improve the thermal properties of primary fiber, while the spinnerette with L/D of 4 does.

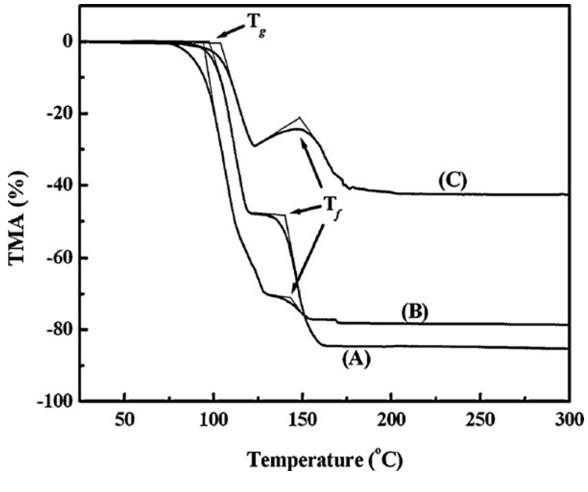

Fig. 3. TMA profiles of primary fibers prepared from liquefied wood with different L/D spinnerettes. (Notes: (A) $L/D=0$; (B) $L/D=2$; (C) $L/D=4$).

3.2. Morphologies observation

The morphologies of primary fibers, which were obtained from melt-spinning at 120 °C with different spinnerettes of $L/D=0$, 2, and 4, were observed by SEM as shown in Fig. 4. Pores with various diameters in cross-section were observed obviously in addition to that splits existed on the fiber surface when spinnerette of $L/D=0$ was applied for preparing primary fiber (Fig. 4(A) and (B)). These defects would be probably caused by not only nitrogen gas which was used for extrusion of spinning solution under gas pressure, but also the spinning nozzle which gave rise to the high value of shear rate of spinning solution at conical die (Fig. 1(A)), and then induced some relaxation of orientation associated with the rough and defective extrudate's surface on primary fiber leaving the orifice (Ahmed, 1982; Zha et al., 1992).

It is well known that the size of the spinnerette hole could influence the quality of extruded filament (Zha et al., 1992). The morphologies of primary fibers were improved after increasing the L/D of spinning nozzle from 0 to 2 and 4. Quite smooth fiber surface and almost no pores existing in cross-section were obtained under the condition of $L/D=4$ (Fig. 4(E) and (F)), while a few splits still remained on the fiber surface in the case of L/D of 2 (Fig. 4(C) and (D)). These results could be explained on the basis of "die swell" or "Barus effect" phenomenon (Kishi & Iizuka, 1964; Malkin, Goncharenko, & Malinovskii, 1976). Pre-entering to cylindrical die of spinnerette, spinning solution with slow flow rate has random conformations in order to minimize entropy. These conformations begin to stretch along the flow direction in response to increase in flow rate caused by flow through narrow cylindrical die. Physical entanglements among molecular chains of spinning solution begin to disentangle proportional to time of polymer under this condition. When exiting cylindrical die, flow returns to slow flow rate, and molecular chains in resultant primary fibers regain the disordered conformations again in order to minimize entropy. Besides, magnitude of die swell is inversely related to the number of disentanglements within the die. Therefore, spinnerette with high L/D value, such as L/D of 4, provided long disentanglement time against relaxation after exiting cylindrical die, which resulted in less die swell and more excellent structure in cross-section and surface of primary fibers (Fig. 4(E) and (F)).

3.3. Pore structure characterization

MIP is a relatively rapid characterization technique for evaluating the pore structure in many porous materials, with which a wide pore diameter range and variety of porosity parameters can be determined (Giesche, 2006; Moura, Ferreira, & Figueiredo, 2005; Vennat, Bogicevic, & Fleureau, 2009; Tatsuo, 2007). In this study, to confirm the various pore structure of primary fibers derived from spinning process under different conditions, MIP measurements were conducted. Total pore surface area, total pore volume, and apparent density of primary fibers prepared from liquefied wood with spinnerettes of $L/D=0$, 2, and 4 are shown in Fig. 5.

It was obvious that the total pore surface area and total pore volume decrease with the L/D of spinnerette increasing. Especially for L/D of 4, only 1.6 m^2/g for total pore surface area and 0.0011 cm^3/g for total pore volume, respectively, were obtained, indicating that

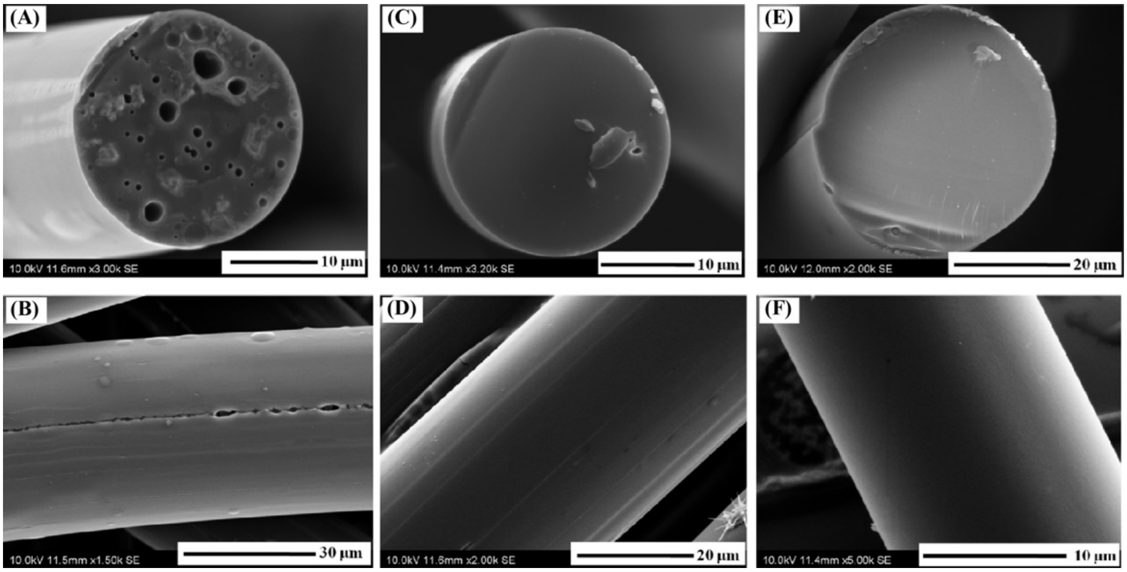

Fig. 4. SEM morphologies of primary fibers prepared from liquefied wood with different *L*/*D* spinnerettes. (Notes: (A and B) *L*/*D* = 0; (C and D) *L*/*D* = 2; (E and F) *L*/*D* = 4).

there were almost no pores occurring in the corresponding primary fibers. Meanwhile, the apparent density of primary fibers showed the inverse trend in comparison with total pore surface area and total pore volume. Therefore, primary fiber prepared from spinnerette with high *L*/*D* exhibited less porous structure and high apparent density. These results are extremely coincident to the results from morphologies observation of primary fibers, further suggesting that it is possible to improve the quality of primary fibers through increasing the *L*/*D* of spinnerette.

3.4. FTIR analysis of primary fibers

FTIR has been proved to be an extremely useful method to investigate the specific interactions between polymers. Fig. 6 illustrates the FTIR spectrums of spinning solution and primary fibers prepared from different spinnerettes of *L*/*D*. In spinning solution spectrum (A), the presence of band centered at around $\nu_{(\mathrm{O–H})} = 3317\,\mathrm{cm}^{-1}$ was assigned to the stretching vibration of hydroxyl groups (Silverstein, Webster, & Kiemle, 2005, chap. 2). After melt-spinning, there was almost no change in the corresponding band shifting of spectrum of primary fiber prepared with spinnerette of *L*/*D* = 0, whereas the bands shifted to the lower wavenumbers of 3282 cm^{-1} and 3180 cm^{-1} upon spinning primary fibers with spinnerette of *L*/*D* = 2 and 4, respectively. This is indicative of more magnitude of hydrogen bonds being formed among phenolic hydroxyl groups of the phenol and/or liquefaction products of lignin by using higher *L*/*D* spinnerette (Kadla & Kubo, 2004; Kubo & Kadla, 2005; Lin, Nakagame, Yao, Yoshioka, & Shiraishi, 2001; Lin, Yao, & Shiraishi, 2001; Silverstein et al., 2005, chap. 2), which could be clearly proved by corresponding effects observed in the O—H in plane bending vibration region (1420–1330 cm^{-1}) (Silverstein et al., 2005, chap. 2).

Additionally, previous studies (Joesten & Drago, 1962; Purcell & Drago, 1967) have shown that the wavenumber shift between the "free" hydroxyl stretching vibration and that of hydrogen bonded species yields a measure of the average strength of the intermolecular interactions, and a linear relationship between the enthalpy of hydrogen bond formation and OH wavenumber shift in phenols exists and can be related by the following equation:

$$-\Delta H(\pm 0.5\,\mathrm{kcal\ mol}^{-1}) = 0.016\Delta\nu_{(\mathrm{O–H})} + 0.63 \qquad (1)$$

Compared with spinning solution, primary fiber prepared with *L*/*D* spinnerette of 0 only $\Delta\nu_{(\mathrm{O–H})} = 2\,\mathrm{cm}^{-1}$, which show $-\Delta H = 0.66\,\mathrm{kcal\,mol}^{-1}$. Whereas in the case of primary fiber

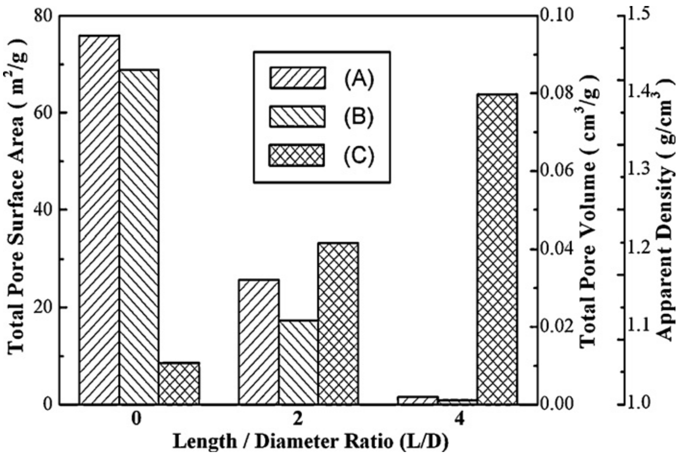

Fig. 5. Total pore surface area (A), total pore volume (B), and apparent density (C) of primary fibers prepared from liquefied wood with different *L*/*D* of spinnerettes.

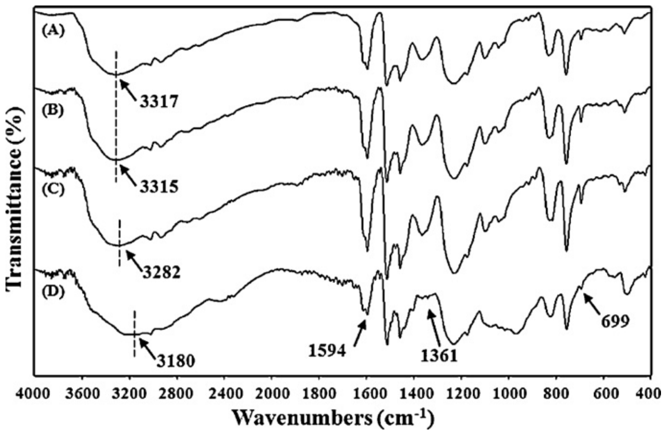

Fig. 6. FTIR spectra of spinning solution and primary fibers prepared from liquefied wood with different *L*/*D* of spinnerettes. (Notes: (A) spinning solution; (B) *L*/*D* = 0; (C) *L*/*D* = 2; (D) *L*/*D* = 4).

prepared with spinnerette of $L/D = 2$ and 4 $\Delta\nu_{(O\text{–}H)} = 35\,\text{cm}^{-1}$, and $137\,\text{cm}^{-1}$, respectively. From the above equation, the extended L/D spinnerette system had an enthalpy of hydrogen bond formation, $-\Delta H = 1.19\,\text{kcal mol}^{-1}$ vs $-\Delta H = 2.82\,\text{kcal mol}^{-1}$ in the primary fibers, suggesting that lower entropy and less "die swell" or "Barus effect" phenomenon of primary fibers can be obtained through hydrogen bond formation by using spinnerette with high L/D. The differences in enthalpy of hydrogen bond formation of primary fibers prepared with different spinnerettes are $0.53\,\text{kcal mol}^{-1}$ (between $L/D = 0$ and $L/D = 2$) and $1.63\,\text{kcal mol}^{-1}$ (between $L/D = 2$ and $L/D = 4$), which are consistent with DTG results (Fig. 2). Wherein the corresponding temperatures of exothermic peaks occurred in DTA curves of $L/D = 4$ are 29 °C and 48 °C greater than those of $L/D = 2$, while difference in temperatures of only 11 °C and 10 °C are obtained between $L/D = 2$ and $L/D = 0$. Accordingly, primary fiber prepared with spinnerette of $L/D = 4$ exhibit best thermal stability, compared with other primary fibers prepared with spinnerette of $L/D = 0$ and 2.

4. Conclusion

The primary fibers prepared from liquefied wood in phenol by melt-spinning with various spinnerettes of L/D exhibited extremely different thermal stability and structural properties. With the L/D of spinnerette increasing, high thermal transition temperatures and low weight loss percentages of resultant primary fibers representing good thermal stability were obtained, as well as less defective structures occurring on the cross section and surface of primary fibers. Especially for $L/D = 4$, there were only total specific surface area of $1.6\,\text{m}^2/\text{g}$ and total pore volume of 0.0011 mL/g being determined. These improvements were the results of the formation of hydrogen bond in the period of flow entering the cylindrical die of spinnerette. Accordingly, the preparation of primary fibers with porous or defect-free structure, which are probably applied for the precursors of activated carbon fibers or carbon fibers with high performance, respectively, can be well conducted by controlling the spinnerette system.

Acknowledgment

Financial support from Forestry Public Special Scientific Research in China (No. 201004057) is gratefully acknowledged.

References

Ahmed, M. (1982). *Textile science and technology, polypropylene fibers-science and technology*. New York: Elsevier., pp. 128–136.

Bright, A. A., & Singer, L. S. (1979). The electronic and structural characteristics of carbon fibers from mesophase pitch. *Carbon*, *17*, 59–69.

Giesche, H. (2006). Mercury porosimetry: A general (practical) overview. *Particle and Particle Systems Characterization*, *23*, 9–19.

Hamada, T., Nishida, T., Furuyama, M., & Tomioka, T. (1988). Transverse structure of pitch fiber from coal tar mesophase pitch. *Carbon*, *26*, 837–841.

Joesten, M. D., & Drago, R. S. (1962). Thermodynamic data for the association of phenol with a series of amides. *Journal of American Chemical Society*, *84*, 2696–2699.

Kadla, J. F., & Kubo, S. (2004). Lignin-based polymer blends: Analysis of intermolecular interactions in lignin–synthetic polymer blends. *Composites: Part A*, *35*, 395–400.

Kishi, N., & Iizuka, H. (1964). The Barus effect of polymer melts. *Journal of Polymer Science Part B: Polymer Letters*, *2*, 399–402.

Kubo, S., & Kadla, J. F. (2005). Hydrogen bonding in lignin: A Fourier transform infrared model compound study. *Biomacromolecules*, *6*, 2815–2821.

Kubo, S., Uraki, Y., & Sano, Y. (1996). Thermomechanical analysis of isolated lignins. *Holzforschung*, *50*, 144–150.

Lee, S. H., Teramoto, Y., & Shiraishi, N. (2002). Resol-type phenolic resin from liquefied phenolated wood and its application to phenolic foam. *Journal of Applied Polymer Science*, *84*, 468–472.

Leon, C. A. L. Y. (1998). New perspectives in mercury porosimetry. *Advances in Colloid and Interface Science*, *76–77*, 341–372.

Lin, L. Z., Nakagame, S., Yao, Y. G., Yoshioka, M., & Shiraishi, N. (2001). Liquefaction mechanism of β-O-4 lignin model compound in the presence of phenol under acid catalysis. Part 2: Reaction behavior and pathways. *Holzforschung*, *55*, 625–630.

Lin, L. Z., Yao, Y. G., & Shiraishi, N. (2001). Liquefaction mechanism of β-O-4 lignin model compound in the presence of phenol under acid catalysis. Part 1: Identification of the reaction products. *Holzforschung*, *55*, 617–624.

Lin, L. Z., Yoshioka, M., Yao, Y. G., & Shiraishi, N. (1995a). Physical properties of moldings from liquefied wood resins. *Journal of Applied Polymer Science*, *55*, 1563–1571.

Lin, L. Z., Yoshioka, M., Yao, Y. G., & Shiraishi, N. (1995b). Preparation and properties of phenolated wood/phenol/formaldehyde cocondensed resin. *Journal of Applied Polymer Science*, *58*, 1297–1304.

Ma, X. J., & Zhao, G. J. (2010). Preparation of carbon fibers from liquefied wood. *Wood Science and Technology*, *44*, 3–11.

Maldas, D., Shiraishi, N., & Harada, Y. (1997). Phenolic resol resin adhesives prepared from alkali-catalyzed liquefied phenolated wood and used to bond hardwood. *Journal of Adhesion Science and Technology*, *11*, 305–316.

Malkin, A. Y., Goncharenko, V. V., & Malinovskii, V. V. (1976). Barus effect of polymer flows through cylindrical and flat dies. *Mechanics of Composite Materials*, *12*, 439–444.

Moura, M. J., Ferreira, P. J., & Figueiredo, M. M. (2005). Mercury intrusion porosimetry in pulp and paper technology. *Powder Technology*, *160*, 61–66.

Purcell, K. F., & Drago, R. S. (1967). Theoretical aspects of the linear enthalpy wavenumber shift relation for hydrogen-bonded phenols. *Journal of American Chemical Society*, *89*, 2874–2879.

Silverstein, R. M., Webster, F. X., & Kiemle, D. J. (2005). *Spectrometric identification of organic compounds* (7th ed.). Hoboken: Wiley.

Tatsuo, Y. (2007). A method to determine lumen volume and collapse degree of pulp fibers by using bottleneck effect of mercury porosimetry. *Journal of Wood Science*, *53*, 516–519.

Uraki, Y., Kubo, S., Nigo, N., Sano, Y., & Sasaya, T. (1995). Preparation of carbon fibers from organosolv lignin obtained by aqueous acetic acid pulping. *Holzforschung*, *49*, 343–350.

Vennat, E., Bogicevic, C., & Fleureau, J. M. (2009). Demineralized dentin 3D porosity and pore size distribution suing mercury porosimetry. *Dental Materials*, *25*, 729–735.

White, J. L., & Buechler, M. (1984). Mesophase mechanisms in the formation of graphitic microstructures. *Preprints: American Chemical Society, Division of Petroleum Chemistry*, *29*, 388–397.

Zha, Q. F., Shi, J. L., Ji, Y., Liu, L., & Qian, S. A. (1992). The effect of composition and process variables on the spinnability of mesophase pitch. *Carbon*, *30*, 739–745.

Zheng, H., Zhou, J., Du, Y., & Zhang, L. (2002). Cellulose/chitin films blended in NaOH/urea aqueous solution. *Journal of Applied Polymer Science*, *86*, 1679–1683.